ELSEVIER

International Journal of Mass Spectrometry 176 (1998) 103–111

Theoretical and mass spectrometric investigations of the formation of calcium fluoride cluster ions

R. Kaschner[a], J.S. Becker[b,*], G. Seifert[c]

[a]*Institut für Festkörperforschung, Forschungszentrum Jülich GmbH, D-52425 Jülich, Germany*
[b]*Zentralabteilung für Chemische Analysen, Forschungszentrum Jülich GmbH, D-52425 Jülich, Germany*
[c]*Technische Universität Dresden, Institut für Theoretische Physik, D-01062 Dresden, Germany*

Received 2 January 1998; accepted 16 March 1998

Abstract

The formation of $Ca_nF_m^+$ cluster ions (n = 1–3, m = 1–4) was investigated by using two different plasma mass spectrometric methods: spark source mass spectrometry and laser ablation inductively coupled plasma mass spectrometry. Both methods give similar abundance distributions of cluster ions, with a maximum ion intensity for the $Ca_2F_3^+$ species. These measurements were interpreted by theoretical calculations of the structures and formation energies of different cluster ions $Ca_nF_m^+$, within density functional theory, using a self-consistent field linear combination of atomic orbitals method. We discuss the possible reaction channels of the cluster formation and find that the formation energies of the clusters correlate with the intensities of the $Ca_nF_m^+$ ions. Qualitatively, clusters with closed electronic shells—in particular, CaF^+ and $Ca_2F_3^+$—are especially stable ("magic" clusters) and show a high abundance in the mass spectrum. (Int J Mass Spectrom 176 (1998) 103–111) © 1998 Elsevier Science B.V.

Keywords: Calcium fluoride; Clusters; Laser ablation inductively coupled plasma mass spectrometry; Spark source mass spectrometry; Density functional theory; Formation energies

1. Introduction

Solid-state mass spectrometric methods [1, 2]—such as spark source mass spectrometry (SSMS), glow discharge mass spectrometry (GDMS), or laser ablation inductively coupled plasma mass spectrometry (LA-ICP-MS)—are sensitive methods for the determination of trace elements in high-purity inorganic materials. The determination of trace and ultra-trace impurities in solid samples using plasma mass spectrometry is sometimes difficult, especially if cluster ions are formed in the plasma, which complicates the analysis of trace elements through isobaric interferences with analyte ions. Therefore, systematic investigations of cluster ion formation can be useful for estimating and correcting such interferences of analyte and cluster ions at the same mass number if low resolution mass spectrometry (e.g. quadrupole mass spectrometry) is used.

Experimental investigations of the cluster ion formation in plasma mass spectrometry have been of interest for more than three decades. In the past 15 years cluster research dramatically increased in the

* Corresponding author.

PII S1387-3806(1898)14020-4

complex fields of cluster physics and cluster chemistry in general [3–7]. Cluster physics viewed these homogeneous aggregates as a link in a chain from atoms or molecules through small crystallites to a complete solid-state structure. As an example of ionic crystals, the evolution of the structure of sodium chloride as a function of the size of $Na(NaCl)_n^+$ clusters has been investigated by Martin [4].

The cluster size distributions as they are observed experimentally are strongly influenced by the experimental conditions, such as temperature, pressure, and so on. Although some qualitative insight can be obtained from nucleation theory, solving kinetic equations [8], or using statistical models [9], the rigorous theoretical prediction of cluster size distributions is practically impossible. But fortunately it was found that the structure in the size distributions—like the appearance of "magic numbers"—in the mass spectra of clusters may be related to the formation energies (stabilities) of the clusters (see e.g. Becker et al. [6] and Galli et al. [10]).

In particular, those clusters with closed electronic shells (i.e. "magic clusters," with saturated bonds, fulfilling the octet rule) have a relatively high stability, which corresponds to a large formation energy and a high abundance in the mass spectrum. The relation among closed (electronic) shells, high stability, and high abundance was successfully applied, especially for alkaline metal clusters and their ions (see e.g. de Heer [7]).

We will show that the concept of closed electronic shells is also useful for the understanding of the stability of clusters of ionic crystals, for example $Ca_nF_m^+$ clusters.

This paper starts with the presentation of the results of experimental investigations on the formation of $Ca_nF_m^+$ cluster ions using two different plasma mass spectrometric methods. The possible reaction channels for the formation of neutral and cationic calcium fluoride clusters and the corresponding formation energies are then obtained theoretically from the binding energies of several optimized clusters. The calculations are performed within density functional theory using a self-consistent field linear combination of atomic orbitals (LCAO) method.

2. Experimental

For the analysis of nonconducting CaF_2 single crystals, solid-state mass spectrometric methods such as SSMS and LA-ICP-MS are well suited. Principles, ion formation processes, and applications of these solid-state mass spectrometric methods in comparison with ICP-MS of aqueous solution are described by Becker and Dietze [11].

SSMS, which analyzes mostly conducting samples, is carried out using a special experimental arrangement for electrodes. The single CaF_2 sample is installed in a Ta holder, whereas the nonconducting sample is sparked using a Ta-counter electrode. The cluster ion distribution of CaF_2 by SSMS—using a double-focusing Mattauch-Herzog-type instrument (MX 3301, St. Petersburg)—was studied at a mass resolution of $m/\Delta m \approx 10{,}000$ under high-vacuum conditions ($<10^8$ Torr).

For LA-ICP-MS, a low-resolution quadrupole mass spectrometer (ELAN 5000, Perkin Elmer, Sciex) was used ($m/\Delta m \approx 300$). The experimental parameters of the mass spectrometric methods used for the investigation of the abundance distribution of cluster ions and for the determination of the purity of the CaF_2 single crystal are summarized in Table 1.

A high-purity single-crystalline CaF_2 sample was investigated mass spectroscopically for measurements of the $Ca_nF_m^+$ cluster ion distribution. In addition, the purity of this CaF_2 single crystal was determined by SSMS in comparison with a double-focusing sector field ICP-MS ("ELEMENT," Finnigan MAT, Bremen, Germany) after microwave-induced acid digestion (with aqua regia using ultrahigh chloride and nitride acid, TAMAPURE-AA-10, Tama Chemicals).

3. Theory

To explain the abundance of different $Ca_nF_m^+$ clusters in the mass spectra experiments, we performed self-consistent density functional calculations for the different clusters. The applied method is an

Table 1
Experimental parameters of mass spectrometric methods for analysis of $Ca_nF_m^+$ cluster ion intensities by SSMS and LA-ICP-MS and for determination of purity of CaF_2 single crystal by SSMS on solid sample in comparison to ICP-MS after sample digestion

Method	Ion source		Ion separation		Ion detection
SSMS	Evaporation and ionization in spark plasma		Double-focusing mass spectrometer (Mattauch-Herzog geometry)		Ion-sensitive photoplate Ilford Q2
	Spark voltage, 60 kV				
	Pulse width, 100 μs		Mass range	8–288 u	
	Repetition frequency, 100 Hz		Mass resolution [$m/\Delta m$]	~10,000	
LA-ICP-MS	Laser ablation and ionization in inductively coupled plasma		Quadrupole mass analyser		Electrical ion detection SEM
	Nd-YAG laser				
	Wavelength	266 nm	Mass range	6–240 u	
	Pulse width	10 ns	Mass resolution range [$m/\Delta m$]	~300	
	Repetition frequency	20 Hz			
	Radiofrequency power	1050 W			
	Coolant gas flow rate	13.5 L min^{-1}			
	Auxiliary gas flow rate	0.7 L min^{-1}			
	Nebulizer gas flow rate	0.80 L min^{-1}			
ICP-MS	Atomization and ionization in inductively coupled plasma		Double focusing mass spectrometer (reverse Nier-Johnson geometry)		Electrical ion detection SEM
	Radiofrequency power	1200 W	Mass range	1–260 u	
	Frequency of generator	27.12 MHz	Mass resolution [$m/\Delta m$]:	300, 3000, 7500	
	Coolant gas flow rate	14 L min^{-1}			
	Auxiliary gas flow rate	0.7 L min^{-1}			
	Nebulizer gas flow rate	1 L min^{-1}			
	Meinhard nebulizer				

LCAO scheme within the local (spin) density approximation [L(S)DA] of density functional theory.

For gradient corrections to the LDA, we performed test calculations and found no significant change of the binding energies. These corrections lead to somewhat (by <10%) smaller binding energies, which does not change the qualitative behavior of the results. (For example, the binding energy with the Becke [12] and Perdew [13] gradient correction is −5.240 eV for CaF, −5.373 eV for CaF^+, and −22.679 eV for $Ca_2F_4^+$. The corresponding LDA values are −5.603, −5.686, and −24.738 eV, respectively; see Table 3.)

We used the code "adf" (Amsterdam density functional) [14], which has the following characteristics. For the wave functions, an LCAO ansatz was used. The basis set used has triple-zeta quality. All integrals were solved numerically with Gauss-Legendre-based integration algorithms, where the space is separated in a special manner. The densities are fitted to a sum of Slater-type functions to simplify the calculation of the multicenter Coulomb integrals.

The geometries of neutral and cationic clusters $Ca_nF_m^{(+)}$ were optimized.

To connect the calculated energies of the clusters with the mass spectra, the assumption is made that a high relative intensity in the mass spectrum is due to a high stability of the cluster and vice versa. For the consideration of the stability, we took into account formation and fragmentation energies for the corresponding reactions

$$A + B \rightleftharpoons C$$

These energies were calculated via

$$\Delta E = E_B(C) - E_B(A) - E_B(B)$$

from the binding energies E_B. The binding energies of the clusters are defined as the difference between the calculated total energy (E_{tot}) of the cluster and the total energies (E_k^{at}) of the isolated atoms (numbered by k):

$$E_B \equiv E_{\text{tot}} - \sum_k E_k^{\text{at}}$$

For the cations the ionization energies were also considered.

As mentioned above, for a quantitative description of cluster abundance versus cluster size, the investigation of nucleation and fragmentation kinetics, including plasma parameters, would be necessary. However, considerations of kinetic equations, as was done e.g. by Bernholc and Phillips [8] for carbon clusters, have shown that the qualitative pattern of the abundance distribution is essentially determined by the energies. Hence, the binding and formation energies of the clusters may be used for the interpretation of the abundance distributions of the clusters in the mass spectra, especially with regard to the absence of several clusters and the high abundance of others ("magic numbers").

4. Results

4.1. Mass spectrometric measurements

In the mass spectrum measured by SSMS and LA-ICP-MS of the CaF_2 single crystal $Ca_nF_m^+$ cluster ions with $n = 1$–3 and $m = 1$–4 were detected. The cluster ion distributions (relative ion intensities: $Ca_nF_m^+/Ca^+$) measured by SSMS are shown in the upper part of Fig. 1. For cluster ions with $n = 1$ and 3, with increasing cluster size the ion intensities decrease. For $Ca_nF_m^+$ clusters with $n = 2$, a local maximum with $m = 3$ was observed. A similar abundance distribution of $Ca_nF_m^+$ cluster ions with a local maximum intensity for $Ca_2F_3^+$ species was detected by LA-ICP-MS (bottom part of Fig. 1).

It is interesting to note, that no $Ca_nF_m^+$ cluster ions were observed in ICP-MS of aqueous solution (after CaF_2 dissolution) because of the loss of fluorine during the microwave digestion.

The determination of relative cluster ion intensities in LA-ICP-MS, which used Ar as carrier and plasma gas, is impossible because of an interference of $^{40}Ar^+$ with $^{40}Ca^+$ (required mass resolution: $m/\Delta m \approx$ 190,000). The other low-abundant Ca isotopes are disturbed by interferences with molecular ions (e.g. $^{44}Ca^+$ with $^{12}C^{16}O_2^+$); therefore, the determination of atomic ions of Ca with low-resolution LA-ICP-MS using a quadrupole analyser is difficult and in Fig. 1 the measured (absolute) cluster ion intensities in LA-ICP-MS are considered. Furthermore, because of interferences of $^{40}Ar^{19}F_{1,2}^+$ and $^{40}Ca^{19}F_{1,2}^+$, the determination of these cluster ions $^{40}Ca^{19}F^+$ and $^{40}Ca^{19}F_2^+$ in LA-ICP-MS is disturbed.

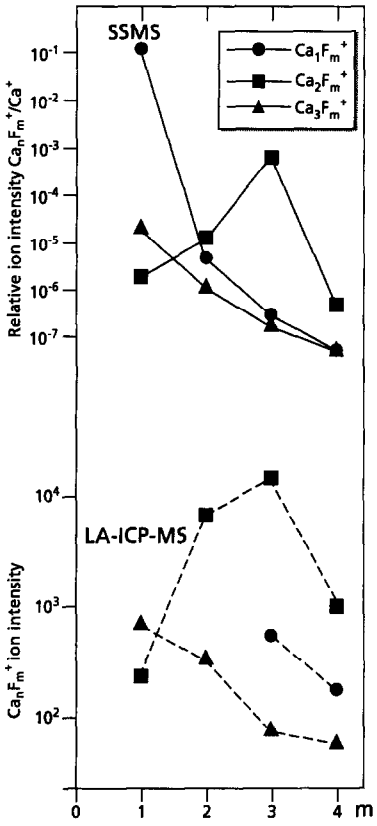

Fig. 1. Abundance distributions of $Ca_nF_m^+$ cluster ions in SSMS and LA-ICP-MS.

The existence of different clusters in mass spectra disturbs the determination of ultratrace elements. The possible interferences of $^{40}Ca_n{}^{19}F_m^+$ cluster ions with atomic ions of the analyte by ultratrace analysis of high-purity CaF_2 are summarized in Table 2. Whereas most interferences of cluster ions and atomic ions of the analyte could be separated in SSMS because of a

Table 2
Possible interferences of cluster ions and atomic ions in mass spectra and required mass resolution for separation

Cluster ion	Mass [u]	Atomic ion of analyte	Required mass resolution ($m/\Delta m$)
$^{40}Ca^{19}F^+$ ($^{40}Ar^{19}F^+$)[a]	58.9610	$^{59}Co^+$	2120
$^{40}Ca^{19}F_2^+$ ($^{40}Ar^{19}F_2^+$)[a]	77.9594	$^{78}Se^+$	1850
$^{40}Ca^{19}F_3^+$	96.9578	$^{97}Mo^+$	1850
$^{40}Ca^{19}F_4^+$	115.9562	$^{116}Sn^+$	2130
$^{40}Ca_2{}^{19}F^+$	98.9236	($^{99}Tc^+$)	
$^{40}Ca_2{}^{19}F_2^+$	117.9220	$^{118}Sn^+$	5790
$^{40}Ca_2{}^{19}F_3^+$	136.9204	$^{137}Ba^+$	9400
$^{40}Ca_2{}^{19}F_4^+$	155.9188	$^{156}Gd^+$	46,850
$^{40}Ca_3{}^{19}F^+$	138.8862	$^{139}La^+$	6840
$^{40}Ca_3{}^{19}F_2$	157.8846	$^{158}Gd^+$	4000
$^{40}Ca_3{}^{19}F_3$	176.8830	$^{177}Hf^+$	2940
$^{40}Ca_3{}^{19}F_4$	195.8814	$^{196}Pt^+$	2350

[a]Observed interference in LA-ICP-MS.

high mass resolution of 10,000, an ultratrace analysis was not possible using a low-resolution quadrupole-based LA-ICP-MS. Furthermore, a quantification of analytical results for ultratrace analysis in solid state mass spectrometry is difficult because of a lack of suitable standard reference materials. A quantification of the analytical results is easy by ICP-MS of aqueous solution using calibration standard solution. Therefore, SSMS (the relative sensitivity coefficients for the elements were defined to be 1) and double-focusing sector field ICP-MS (after dissolution of the sample) were compared in order to determine the ultratrace impurities in high-purity CaF_2. Possible interferences of molecular ions with cluster ions could be separated using high mass resolution in both mass spectrometric methods. The purity of the investigated CaF_2 single crystal was determined by both methods to be 99.996%.

4.2. Calculations

The results (geometries and energies) for the optimized cationic clusters $Ca_nF_m^+$ for $n = 1, 2$ and $m = 1$–4 and for the corresponding neutral clusters are given in Table 3. The binding energies of the cations $Ca_nF_m^+$ are given with respect to

$$Ca_nF_m^+ \rightarrow Ca^+ + (n-1)\,Ca + m\,F$$

Table 3
Calculated ground state geometries (symmetries), Ca–F bond lengths (in angstroms), and binding energies (E_b, in electronvolts) of the clusters Ca_nF_m and $Ca_nF_m^+$

n	m	Symmetry	r_{Ca-F}	E_b
Neutral clusters				
1	1	$C_{\inf v}$	2.10	−5.603
1	2	$D_{\inf h}$	2.09	−12.546
1	3	D_{3h}	2.12	−15.179
1	4	T_d	2.23	−16.896
2	1	C_{2v}	2.20	−7.128
2	2	D_{2h}	2.21	−14.346
2	3	D_{3h}	2.23	−21.216
2	4	D_{4h}	2.26	−26.912
Cations				
1	1	$C_{\inf v}$	2.03	−5.686
1	2	$D_{\inf h}$	2.19	−7.925
1	3	D_{3h}	2.26	−9.349
1	4	D_{4h}	2.28	−10.466
2	1	C_{2v}	2.16	−8.498
2	2	D_{2h}	2.20	−15.506
2	3	D_{3h}	2.21	−22.813
2	4	D_{4h}	2.26	−24.738

which is the energetically most favored dissociation channel of these cations. This can be understood easily by comparing the strongly different ionization potentials of Ca and F, 6.433 eV and 19.823 eV, respectively.

The ground state structures as obtained by geometry optimization are as follows (see Fig. 2): CaF_2 and CaF_2^+ are linear (F–Ca–F); CaF_3 and CaF_3^+ have Ca in the middle of a equilateral triangle with the F atoms at its corners. CaF_4 has a tetrahedral structure with Ca in the center of the tetrahedron and the F atoms at its corners; CaF_4^+ has a quadratic planar structure. Ca_2F and Ca_2F^+ have a bent structure (Ca–F–Ca); Ca_2F_2 and $Ca_2F_2^+$ are rhombic. Ca_2F_3 and $Ca_2F_3^+$ are trigonal bipyramids with Ca on the tops and an equilateral triangle of the fluorine atoms. The structure of $Ca_2F_4^{(+)}$ is similar to that of $Ca_2F_3^{(+)}$, but a quadratic bipyramid (respectively).

As can be further seen from Table 3, the Ca–F bond length increases with the number of F atoms, except with the CaF_2 cluster, which has a shorter Ca–F bond length than CaF. The shortest distances appear for CaF_2 and CaF^+, which can be understood

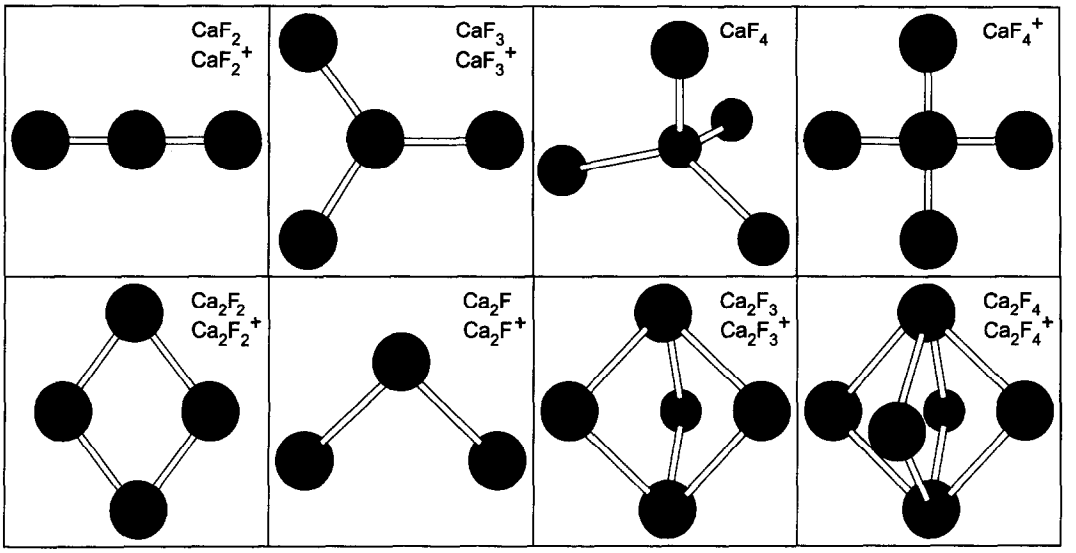

Fig. 2. Equilibrium structures of the clusters (qualitatively).

because these clusters are closed-shell systems according to the octet rule. Similarly, the closed-shell system $Ca_2F_3^+$ has a Ca–F bond length only marginally larger than in $Ca_2F_2^+$. Generally, the Ca–F bond lengths in the clusters are considerably shorter than in crystalline CaF_2, where $r_{Ca-F} = 2.365$ Å [15].

The outstanding role of closed-shell clusters as "magic clusters" can also be seen from the binding energies given in Table 3. The binding energy is increased by nearly 7 eV, going from CaF to CaF_2, whereas the addition of further fluorine atoms increases the binding energy only by ~3 eV ($CaF_2 \rightarrow CaF_3$) and ~2 eV ($CaF_3 \rightarrow CaF_4$), respectively. This means that there is a saturation effect in binding fluorine atoms to Ca. A very similar behaviour can be seen for the cations.

This "saturation effect" already qualitatively explains the trends in the abundance distributions in the mass spectra (Fig. 1). For CaF_m^+ the intensity continuously decreases with an increasing number of F atoms; and CaF^+—the closed-shell system in this series—has a rather high intensity. In the $Ca_2F_m^+$ series, Ca_2F^+ has a rather low intensity. The intensity increases with the increasing number of F atoms up to $Ca_2F_3^+$, the "saturated" closed-shell system in this series.

This rough qualitative picture may be improved by the consideration of the reaction energies of possible cluster formation reactions. There are plenty of possible reaction paths for the formation of the clusters and cluster ions.

Because of the small binding energies of calcium as well as fluorine clusters and their cations, the appearance of these clusters in the plasma is very improbable. The same certainly also holds for F^+, because of the very large ionization energy of fluorine.

The reaction paths via the anion F^- and via the simple ionization of the neutral Ca_nF_m clusters is discussed separately (see below). Consequently, the clusters should be preferably formed from atoms and ions F, Ca, and Ca^+, and a very probable way to build up the cationic clusters should be (see the following discussion of Fig. 4):

$$CaF_m^+ + F \rightarrow CaF_{m+1}^+ (m = 0\text{–}3)$$

$$CaF^+ + Ca \rightarrow Ca_2F^+$$

$$Ca_2F_m^+ + F \rightarrow Ca_2F_{m+1}^+ (m = 1\text{–}3)$$

The energies of all these reactions can be determined simply from the values of Table 3, considering

Table 4
Reaction (formation) energies E_f (in electronvolts) of all cationic clusters $Ca_nF_m^+$

n	m	E_f
1	1	−5.69
1	2	−2.24
1	3	−1.42
1	4	−1.12
2	1	−2.81
2	2	−7.01
2	3	−7.31
2	4	−1.93

also the ionization energy of Ca. The resulting reaction (formation) energies are given in Table 4 and Fig. 3; the negative signs mean that the reactions are exothermic.

The calculated size dependence of the formation energies for the CaF_m^+ and $Ca_2F_m^+$ series (Fig. 3) looks very similar to the corresponding size dependences of both measured abundance distributions (Fig. 1). Furthermore, the theoretical results confirm the "saturation effect" in the cluster growth, as discussed above, on the basis of the binding energies. For CaF_m^+ the gain in energy becomes smaller with increasing m, because the closed-shell system ("saturated cluster") for the cation is already reached with $m = 1$. For $Ca_2F_m^+$, "saturation" occurs for $m = 3$ (which is again the closed-shell system), corresponding to the maximum of the formation energy in that series (Fig. 3) or to the maximum of the measured intensities in the mass spectra (Fig. 1).

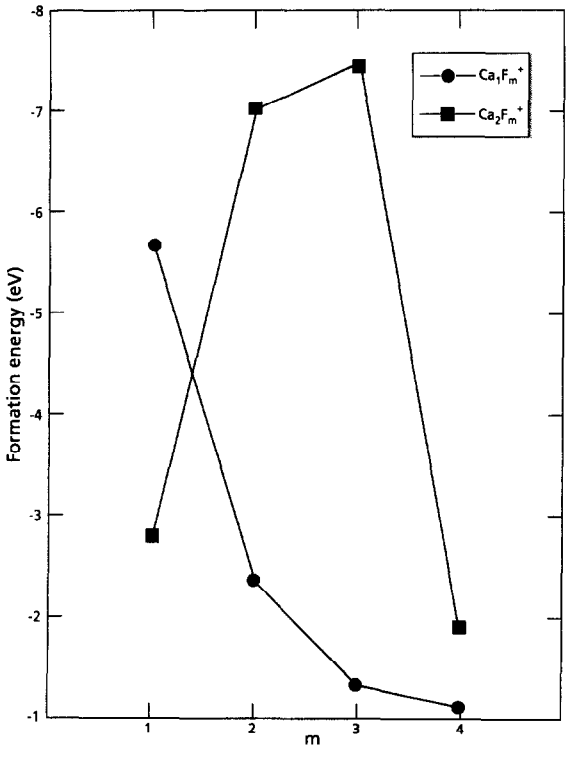

Fig. 3. Calculated formation energies of $Ca_nF_m^+$ cluster ions.

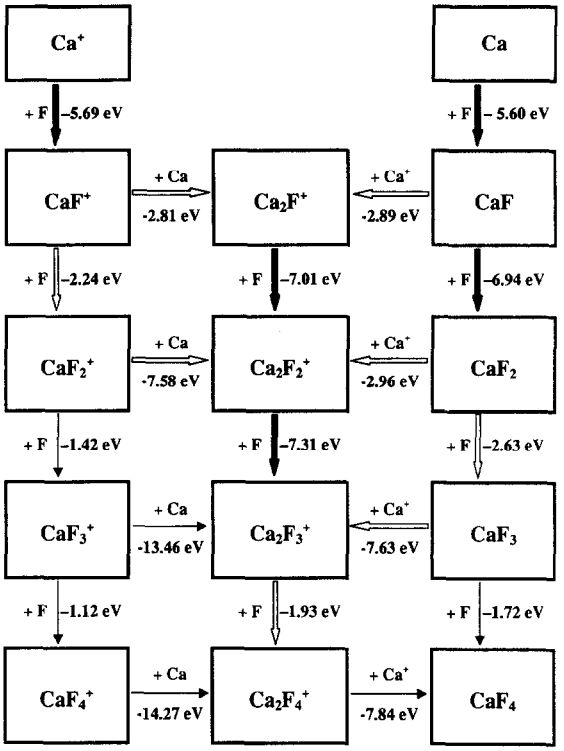

Fig. 4. Scheme of possible reaction/formation channels of Ca_nF_m clusters and cluster cations. The reaction energies are given in electronvolts. The dominating paths are indicated by bold and double-line arrows.

To show the reliability of these results, we also calculated the reaction energies of the other possible reaction channels, i.e. excluding the channels via F_2, F^+, F^-, Ca_2, and Ca_2^+ (see above). These formation energies lead to a scheme of possible ways for cluster formation, as illustrated in Fig. 4.

The conclusions are the following—using the fact

that the reaction energy and the concentration of the input molecules are related to the probability of the corresponding reaction (see Sec. 3).

There are only a few probable reactions in addition to those considered in Table 4: Ca_2F^+ may also be formed by CaF + Ca^+, but the reaction energy for this (−2.89 eV) is almost the same as for the reaction CaF^+ + Ca. The formation of $Ca_2F_2^+$ is also possible from CaF_2^+ and CaF_2; however, the energy gains for these reactions (−7.58 and −2.96 eV, respectively) are comparable to or smaller than the energy given in Table 4 (−7.01 eV). $Ca_2F_3^+$ may also be formed from CaF_3 with a similar reaction energy (−7.63 eV) as above (−7.31 eV). However, $Ca_2F_3^+$ does not significantly arise from CaF_3^+ because CaF_3^+ is relatively rare, because its formation energy (more precisely, the absolute value of this energy) is relatively low. For similar reasons, $Ca_2F_4^+$ should only arise from the reaction considered above (Table 4).

In addition to Fig. 4, two further reaction channels could be possible.

(1) The neutral clusters CaF_m may also be formed via F^- by the reaction

$$CaF_m^+ + F^- \rightarrow CaF_{m+1} (m = 0\text{–}3)$$

Our calculations show that these reactions are strongly exothermic (≈9 eV) for all values of m, but these large reaction energies have only a small variation with m. Hence, these charge neutralization reactions will not lead to a characteristic size dependence pattern in the abundance distribution of Ca_nF_m clusters. Consequently, this will not change the conclusions as discussed above by considering only CaF_m + F → CaF_{m+1} (m = 0–3).

(2) The cationic clusters may also be formed by a simple ionization of the corresponding neutral species due to collisions with electrons:

$$Ca_nF_m \rightarrow Ca_nF_m^+ + e^-$$

The calculated ionization energies of Ca_nF_m clusters are shown in Table 5.

From Table 5 one can see that stable neutral clusters (e.g. CaF_2) have large ionization energies, whereas the ionization energies of clusters with corresponding stable cations (CaF^+, $Ca_2F_3^+$) are small. This means that these cluster cations may also be formed easily by ionization of the corresponding neutral clusters, Therefore, possible ionization of neutral clusters formed in the plasma will additionally increase the abundance of the closed-shell cluster cations (especially of CaF^+, compared with the other clusters CaF_m^+).

Table 5
Calculated ionization energies (I_P, in electronvolts) for the transition $Ca_nF_m \rightarrow Ca_nF_m^+$; from the values of Table 3[a]

n	m	I_P
1	1	6.367
1	2	11.054
1	3	12.263
1	4	12.863
2	1	5.062
2	2	5.273
2	3	4.836
2	4	6.606

[a]Note that for I_P the binding energies of the cationic clusters have to be considered with respect to the *neutral* atoms. This causes a difference of 6.433 eV (i.e. the ionization energy of Ca) compared with the binding energies for the cations in Table 3.

Finally, the case n = 3 is discussed briefly. For these clusters we did not perform density-functional calculations because of the vast variety of possible isomers. However, the measured abundances, which monotonically (and slowly) decrease with m, can be understood by applying the results for the cases with n < 3 (see above). There is no value m (≤4), for which the cluster fulfills the octet rule. Hence, the addition of further F atoms does not yield a significant enhancement of the stability of the clusters, and the addition of more F atoms leads to a decreasing energy gain for increasing m, at least for the considered size range in the measurements ($m \leq 4$).

5. Conclusions

We measured the abundances of $Ca_nF_m^+$ clusters (for n = 1–3 and m = 1–4) by SSMS and LA-ICP-MS. Both methods yield similar results. No $Ca_nF_m^+$ cluster ions were observed in ICP-MS of aqueous solution after digestion of a high-purity CaF_2

sample because of the loss of fluorine during the microwave-induced acid digestion.

The mass spectrometric measurements of the cluster distributions of the $Ca_nF_m^+$ species were interpreted by theoretical calculations, using a self-contained field LCAO code within density functional theory. From the binding energies of several neutral and cationic calcium fluoride clusters we obtained the formation energies of the cations for all possible reaction channels. These energies are a measure of the stability of the clusters and agree nicely with the trends of the abundances in the mass spectra.

Quantitative predictions of cluster abundances from plasma sources as a function of plasma parameters still need further theoretical investigations. Especially the kinetics/dynamics of the formation and fragmentation processes have to be considered. However, a solution can hardly be seen for this complex problem at present.

Acknowledgements

The authors would like to thank A.I. Saprykin (Institute of Inorganic Chemistry, Novosibirsk) and D. Tenzler (Research Centre Jülich) for experimental investigations on CaF_2 single crystals.

References

[1] F. Adams, R. Gijbels, R. van Grieken (Eds.), Inorganic Mass Spectrometry, Chemical Analysis, Wiley, New York, 1988, Vol. 95.
[2] J.S. Becker, H.-J. Dietze, Int. J. Mass Spectrom. Ion Processes 164 (1997) 89.
[3] T.D. Märk, Adv. Mass Spectrom. 13 (1995) 71.
[4] T.P. Martin, in H. Haberland (Ed.), Clusters of Atoms and Molecules, Springer, Berlin, 1994.
[5] J.S. Becker, H.-J. Dietze, J. Fresenius, Anal. Chem. 359 (1997) 338.
[6] J.S. Becker, G. Seifert, A.I. Saprykin, H.-J. Dietze, J. Anal. At. Spectrom. 11 (1996) 643.
[7] W. de Heer, Rev. Mod. Phys. 65 (1993) 611.
[8] J. Bernholc, J.C. Phillips, J. Chem. Phys. 85 (1986) 3258; Phys. Rev. B 33 (1986) 7395.
[9] O. Knospe, R. Schmidt, G. Seifert, Phys. Lett. A 129 (1988) 236.
[10] G. Galli, W. Andreoni, M.P. Tosi, Phys. Rev. A 34 (1986) 3580.
[11] J.S. Becker, H.-J. Dietze, Spectrochim. Acta B (in press); Report of Research Centre Jülich, JÜL-3468 (1998) 1.
[12] A.D. Becke, Phys. Rev. A 38 (1988) 3098.
[13] J.P. Perdew, Phys. Rev. B 33 (1986) 8822.
[14] (a) P.M. Boerrigter, G. te Velde, E.J. Baerends, Int. J. Quantum Chem. 33 (1988) 87; (b) G. te Velde, E.J. Baerends, J. Comput. Phys. 99 (1992) 84 and references therein.
[15] Landolt-Börnstein, Zahlenwerte und Funktionen aus Naturwissenschaft und Technik, Vol. III/7a, Springer-Verlag, Berlin, 1973.